

See discussions, stats, and author profiles for this publication at: <https://www.researchgate.net/publication/236205208>

Enhanced Physical and Oxidative Stabilities of Soy Protein-Based Emulsions by Incorporation of a Water-Soluble Stevioside-Resveratrol Complex

ARTICLE in JOURNAL OF AGRICULTURAL AND FOOD CHEMISTRY · APRIL 2013

Impact Factor: 2.91 · DOI: 10.1021/jf4003945 · Source: PubMed

CITATIONS

21

READS

63

5 AUTHORS, INCLUDING:



Zhili Wan

South China University of Technology

15 PUBLICATIONS 81 CITATIONS

SEE PROFILE

Enhanced Physical and Oxidative Stabilities of Soy Protein-Based Emulsions by Incorporation of a Water-Soluble Stevioside–Resveratrol Complex

Zhi-Li Wan,[†] Jin-Mei Wang,[†] Li-Ying Wang,[†] Xiao-Quan Yang,^{*,†,‡} and Yang Yuan[†]

[†]Research and Development Center of Food Proteins, Department of Food Science and Technology, and [‡]State Key Laboratory of Pulp and Paper Engineering, South China University of Technology, Guangzhou 510640, People's Republic of China

S Supporting Information

ABSTRACT: To strengthen the effectiveness of resveratrol (RES) as a natural antioxidant in food systems, this work attempted to enhance the water solubility of RES by utilizing the solubilizing properties of stevioside (STE) and investigated the effect of STE-solubilized RES (STE–RES) incorporation on the stability of soy protein isolate (SPI)-based emulsions. The physical properties and oxidative stability of SPI emulsions with STE/STE–RES were evaluated. The water solubility of RES increased with the increase of STE concentration up to its critical micelle concentration, suggesting the solubilization of hydrophobic RES in STE self-assembled micelles. STE micelles competitively adsorbed at the oil–water interface with SPI, forming a mixed SPI and STE interfacial layer, thus resulting in a decrease in particle size and evident enhancement in the physical stability of SPI-based emulsions. After the incorporation of STE–RES, SPI emulsions showed an enhanced oxidative stability with reduced lipid hydroperoxides and volatile hexanal. This improvement was believed to be mainly attributed to the targeted migration of RES to the interface during the adsorption of the STE–RES complex, as evidenced by high interfacial accumulation of RES.

KEYWORDS: resveratrol, stevioside, soy protein isolate, oil/water emulsion, physical stability, oxidative stability

INTRODUCTION

Lipid oxidation in foods and biological systems has been a major cause for both food-quality deterioration and health complications. The oxidative degradation of lipids causes unpleasant quality changes in food, such as the development of unpalatable flavors and odors, loss of nutritional values, color changes, and even formation of potentially toxic reaction products.^{1,2} Lipids in the oil-in-water (O/W) emulsions are believed to be highly susceptible to oxidation because the higher interfacial area of emulsions may promote interactions between lipids and pro-oxidants in the aqueous phase.^{1,3} Therefore, exogenous antioxidants are usually incorporated into O/W emulsions to enhance their oxidative stability. Moreover, the accumulation of antioxidants at the oil–water interface is expected to promote their antioxidant effectiveness in emulsion systems.^{1,4} Currently, special attention is focused on the use of natural polyphenolic compounds to retard lipid oxidation due to their safety as food ingredients and remarkable antioxidant activity.⁵

Resveratrol (*trans*-3,5,4'-trihydroxystilbene, RES; Figure S1 in the Supporting Information) is a natural polyphenol compound found in red grapes and peanuts, as well as a variety of other plant sources. Clinical studies have demonstrated that RES exerts many different health-promoting effects, including antioxidant, anti-inflammatory, anticancer, antiplatelet aggregation, cardioprotective, and antiobesity effects.⁶ The high antioxidant capacity of RES has been verified by inhibition of lipid peroxidation induced by different systems, such as ADP and NADPH in rat liver microsomes,⁷ the ferric thiocyanate (FTC) method,⁸ the Rancimat method,⁹ and other in vitro assays.^{10,11} Medina et al.¹² reported that resveratrol as a food

antioxidant showed good antioxidant activity in fish oil-in-water emulsions and fish muscle, as good as the potent antioxidant hydroxytyrosol. However, RES behaved as a weak antioxidant against oxidation of rapeseed and sunflower oils and also had a low efficiency in margarine (water-in-oil emulsion).¹³ Medina et al.¹² speculated that this discrepancy in antioxidant effectiveness of RES in emulsions may be attributed to the difference in the quantity of its incorporation in oil droplets' surface. In fact, the poor solubility of RES in aqueous and lipid phases limits its application in the field of functional foods as an antioxidant, especially in the emulsified systems, due partly to the unpredictable physical location of RES.^{14,15}

In recent years, several strategies have been attempted to improve the water solubility and bioavailability of RES, such as complexation with cyclodextrin and its derivatives or using bile acid micelle, nanoemulsion, microemulsion, and nanoparticle delivery systems.^{14,16–18} However, significant improvement of RES water solubility remains an elusive goal, although each has made advancements. Recently, Liu et al.¹⁹ reported that natural steviol glycosides, such as rubusoside, could effectively enhance the solubility of various bioactive compounds with poor water solubility by the formation of nanoparticles, including curcumin, paclitaxel, capsaicin, cyclosporine, nystatin, and erythromycin.

Stevioside (STE; Figure S1 in the Supporting Information), the most abundant component of steviol glycosides, probably

Received: January 26, 2013

Revised: April 7, 2013

Accepted: April 16, 2013

Published: April 16, 2013

can display a similar solubilizing effectiveness for water-insoluble RES. To date, STE has been mainly used as a noncaloric natural sweetener in food products due to its intense sweetness (250–300 times sweeter than sucrose).²⁰ STE also exhibits many biological effects on humans, such as antihyperglycemic, antihypertensive, antitumor progression, and immunomodulatory activities.^{21–24} However, there is very little information on the solubilization for water-insoluble polyphenols by using STE. On the other hand, it is very important to note that the amphiphilic structure of STE molecules, similar to that of triterpenoid saponins, may determine their potential capability as natural surface-active substances (biosurfactants) to adsorb at the oil–water interface. Considering the potential surface activity of STE, we thus postulated that the incorporation of STE-solubilized RES (STE–RES) in an O/W emulsion system may result in the targeted accumulation of RES at the oil–water interface owing to the simultaneous adsorption with STE at the droplet surface during the homogenization process. This speculation would lead to an increase in the interfacial resistance to lipid oxidation of emulsions.^{1,4}

In this study, soy protein isolates (SPI) were first selected as effective emulsifiers and stabilizers due to their high nutritional value and excellent functional properties. To strengthen the effectiveness of RES as an antioxidant in protein-based O/W emulsion, we attempted to enhance the water solubility of RES and to purposefully accumulate RES at the oil–water interface in emulsions by uniquely utilizing the solubilizing properties of STE and its surface activity. The effect of STE on the water solubility of RES was investigated, and the underlying solubilization mechanism for RES was also proposed. The physical properties (particle size distribution, physical stability, and interfacial adsorption fraction) and oxidative stability of emulsions stabilized by SPI and STE/STE–RES were evaluated using lipid hydroperoxide measurement and headspace hexanal analysis. In addition, the interactions between SPI and STE/STE–RES in aqueous solutions were investigated using fluorescence quenching studies to understand the enhancement mechanism of emulsion stability.

MATERIALS AND METHODS

Materials. RES (purity > 98%) was purchased from Shanxi Tianrun Phytochemical Co., Ltd., China. STE (purity > 95%) was purchased from Jining Aoxing Stevia Products Co., Ltd., China. Pyrene was purchased from Sigma-Aldrich (St. Louis, MO, USA). Defatted soy flour was provided by Shandong Yuwang Industrial and Commercial Co., Ltd., China. SPI was prepared as described by Wang et al.²⁵ The protein content of SPI was 88.79%, determined by using the Dumas method ($N \times 5.71$, wet basis) in a Rapid N Cube (Elementar France, Villeurbanne, France). Corn oil was purchased from a local supermarket and used without further purification. All other chemicals used were of analytical grade.

Preparation of Water-Soluble RES with STE. Appropriate amounts of RES and STE were mixed in water to make a dispersion in which the concentration of RES was kept constant at 1 mg/mL. The dispersion was stirred gently for 1 h at room temperature (22 °C), to dissolve the mixture. The resulting mixture was incubated at 60 °C in a water bath (TW12; Julabo, Seelbach, Germany) for 30 min. After incubation, all of the samples were protected from light and kept at room temperature (22 °C) for 24 h to equilibrate. Each sample was filtered through a 0.45 μ m filter (Millipore, Billerica, MA, USA) prior to HPLC determination. Quantitative analysis of RES was performed with a reversed-phase Symmetry C18 HPLC column (5 μ m, 3.9 \times 150 mm) using an HPLC system (Waters, Milford, MA, USA) equipped with a Waters 1525 pump and Waters 2487 UV detector. The

separation was done using an isocratic flow of acetonitrile and water (40:60, v/v) at room temperature (22 °C). The flow rate was 0.6 mL/min, and the injection volume was 10 μ L. The UV–visible detector was set at 306 nm for RES detection. The concentration of RES was calculated using a standard curve made from RES dissolved in mobile phase solution.

Critical Micelle Concentration (CMC) Measurement of STE.

The CMC of STE was determined by using the fluorescence probe technique with pyrene as a fluorescence probe.^{26,27} Aliquots of pyrene solution (6.0×10^{-6} M in acetone, 1 mL) were added to vials, and the acetone was allowed to evaporate under a stream of nitrogen. STE solutions (10 mL) at varied concentrations were added into the vials and left to equilibrate overnight at room temperature (22 °C). The final concentration of pyrene in each sample was 6.0×10^{-7} M. The excitation wavelength was 335 nm, and the emission spectrum between 350 and 500 nm was recorded. The excitation and emission slit widths were set at 5 and 2.5 nm, respectively. The intensity ratios of I_{373} to I_{385} were plotted as a function of logarithm of the STE concentrations. The data were fitted using the nonlinear fitting with Boltzman's curve. The CMC was obtained from the inflection point of the nonlinear fitting.

Fluorescence Spectroscopy Measurement. The fluorescence spectra were recorded using an F7000 fluorescence spectrophotometer (Hitachi Co., Japan). Protein intrinsic fluorescence was measured at constant SPI concentration (0.5 mg/mL) and different STE/STE–RES concentrations in 10 mM phosphate buffer (pH 7.0). Emission spectra were recorded from 300 to 500 nm at an excitation wavelength of 280 nm. Both the excitation and emission slit widths were set at 5 nm. The fluorescence spectra of the phosphate buffer were subtracted from the respective spectra of the samples. Fluorescence quenching is described according to the Stern–Volmer equation (eq 1):²⁸

$$F_0/F = 1 + k_0 k_q \tau_0 [Q] = 1 + K_{SV} [Q] \quad (1)$$

In this equation F_0 and F are the fluorescence intensities in the absence and presence of a quencher, respectively, $[Q]$ is the quencher concentration, K_{SV} is the Stern–Volmer quenching constant, k_q is the bimolecular quenching rate constant, and τ_0 is the lifetime of fluorescence in the absence of a quencher. Hence, eq 1 was applied to determine K_{SV} by linear regression of a plot of F_0/F versus $[Q]$.

Emulsion Preparation. O/W emulsion was prepared by dispersing 10 wt % corn oil in a 10 mM phosphate buffer (pH 7.0) containing 0.5% (w/v) SPI. STE–RES and STE alone were added into the SPI/phosphate buffer aqueous phase prior to homogenization, respectively. In all of the emulsions containing STE–RES (0.005–0.02%, w/v), STE concentration was constant at 0.8% (w/v), which was sufficient to solubilize RES and also above its CMC. Emulsions without the addition of STE–RES and STE were used as control samples. Coarse emulsions were prepared using an Ultra-Turrax T25 (IKA-Werke GmbH & Co., Germany) at 6000 rpm for 2 min. Fine emulsions were prepared by passing coarse emulsions twice through an M-110EH-30 microfluidizer processor (Microfluidics, Newton, MA, USA) at 400 bar. After the emulsification process, the pH of each prepared emulsion was measured and adjusted to pH 7.0 with 0.1 or 1 M HCl or NaOH. Sodium azide (0.02 wt %) was then added to the emulsions to prevent microbial growth. Emulsions were placed in lightly sealed screw-cap vials and stored in a dark oven at 37 °C for 21 days.

Mean Particle Size and Microstructure of Emulsions. The mean particle size and size distribution of emulsions were measured by a Mastersizer 2000 (Malvern Instruments Co. Ltd., Worcestershire, UK) at 25 °C. The refractive indices of corn oil and phosphate buffer were taken as 1.467 and 1.330, respectively. The absorption index was 0.001. The particle sizes measured are reported as the volume-weighted mean diameter $d_{43} = \sum n_i d_i^4 / \sum n_i d_i^3$, where n_i is the number of particles with diameter d_i . The microstructure of emulsions was studied using a confocal laser scanning microscope (CLSM, Leica Microsystems Inc., Heidelberg, Germany) with a 100 \times oil immersion objective lens. Aliquots (1 mL) of emulsion were mixed with 40 μ L of staining solution containing 0.1% (w/v) Nile Red (fluorescent dye).

The stained emulsions (50 μL) were placed on concave confocal microscope slides and examined using an argon krypton laser (ArKr, 488 nm).

Determination of Protein and RES at the Oil–Water Interface. The concentration of protein adsorbed at the oil–water interface was determined according to the method described by Akhtar et al.²⁹ with some modifications. Freshly prepared emulsions were centrifuged at 15000g for 2 h at 20 °C using a himac CS150NX micro ultracentrifuge with an S140AT rotor (Hitachi Koki Co. Ltd., Tokyo, Japan). After centrifugation, the subnatants were carefully removed using a syringe and filtered through a 0.45 μm filter (Millipore). The amount of unadsorbed protein remaining in subnatants was determined according to the micro-Kjeldahl method ($N \times 5.71$). The interfacial protein proportion was calculated from the difference between the amount of protein used to prepare the emulsion and that measured in the subnatants after centrifugation. Determination of the distribution of RES in the emulsions was performed according to the procedure described by Panya et al.³⁰ The emulsions were centrifuged as above, and the amounts of RES in subnatants were determined by HPLC system (Waters).

Lipid Hydroperoxide and Hexanal Measurements. Lipid hydroperoxide was measured according to the method described by Tong et al.³¹ with some modifications. Emulsion (0.2 mL) was mixed with 1.5 mL of isooctane/2-propanol (3:1, v/v) and vortexed (10 s, three times). After centrifugation at 1000g for 2 min, the organic solvent phase (200 μL) was added to 2.8 mL of methanol/1-butanol (2:1, v/v), followed by 15 μL of 3.94 M ammonium thiocyanate and 15 μL of ferrous iron solution (prepared by mixing 0.132 M BaCl_2 and 0.144 M FeSO_4). Twenty minutes later, the absorbance was measured at 510 nm using a UV–vis spectrophotometer (Genesys 10, Thermo Scientific, USA). Hydroperoxide concentrations were determined using a standard curve made from hydrogen peroxide.

Fresh emulsion samples (8 mL) were transferred into special 10 mL headspace vials and sealed with silicone rubber Teflon caps with a crimper. After storage in a dark oven at 37 °C for 21 days, headspace hexanal was measured using a Trace DSQ II GC/MS (Thermo-Fisher Scientific, USA) according to the method of Panya et al.³⁰ with some modifications. A 75 μm carboxen/polydimethylsiloxane (Carboxen/PDMS) stable flex solid phase microextraction (SPME) fiber (Supelco, Bellefonte, PA, USA) was inserted through the vial septum and exposed to the sample headspace for 10 min at 55 °C. The SPME fiber was desorbed at 250 °C for 3 min in the GC detector at a split ratio of 1:10. The chromatographic separation was performed using a TR-5MS capillary column (30 m; 0.25 mm i.d.; 0.25 μm film thickness). The temperatures of the oven, injector, and flame ionization detector were 60, 250, and 250 °C, respectively. Sample run time was 15 min. The analysis was carried out on the basis of the results obtained from three replicates of each emulsion sample.

Statistical Analysis. All measurements were carried out in triplicate. An analysis of variance (ANOVA) of the data was performed using the SPSS 13.0 statistical analysis system. Treatments were considered to be significantly different at $p < 0.05$.

RESULTS AND DISCUSSION

Water Solubility Enhancement of RES in STE Micelles.

Figure 1 shows the image of RES dispersions and RES solubility in aqueous solution as a function of STE concentration. RES dispersion appeared very turbid without STE (Figure 1, inset). More RES was dissolved into the water solution and the RES dispersion became more transparent with increasing STE concentration, indicating the solubilization of hydrophobic RES (Figure 1, inset). The solubility of RES quantitatively supported this observation (Figure 1). The solubility of RES in water without STE was only about 22.9 $\mu\text{g}/\text{mL}$. There is no significant increase ($p > 0.05$) in RES solubility until the STE concentration was increased to 0.5% (w/v). With further increasing STE concentration, a linear enhancement of RES solubility was observed. In the presence of 4% STE (w/v), RES

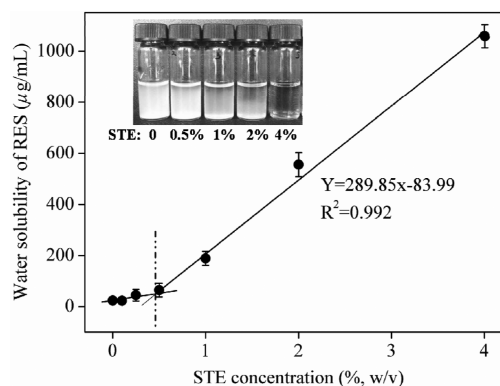


Figure 1. Water solubility profiles of RES with increasing STE concentrations. (Inset) Images of RES dispersion with different STE concentrations.

was solubilized in water to about 1028.4 $\mu\text{g}/\text{mL}$, representing an evident increase in water solubility of RES of about 45 times compared with that of RES without STE. Additional experiments were performed, and a clear aqueous solution of as high as 14 mg/mL RES in 50% STE solution (w/v) (data not shown) was obtained. This high solubility displayed by STE may be comparable with or exceed most cyclodextrins and cyclodextrin derivatives commonly used for the solubilization of RES.³² In addition, dynamic light scattering (DLS) and atomic force microscopy (AFM) analyses demonstrated that the morphology of STE-solubilized RES (STE–RES) was primarily spherical particles with a hydrodynamic diameter of 4.70 nm (data not shown).

STE is a diterpene ent-kaurene glycoside possessing both a hydrophobic steviol backbone and hydrophilic glucosyl and sophorosyl residues (Supporting Information, Figure S1). The amphiphilic structure of STE could make it capable of forming micelles in water. The STE molecule has the shape of a bolaform amphiphile-hydrophobic ring in the center with two hydroxyl groups on each end (Figure S1 in the Supporting Information). Thus, it is reasonable to speculate that the STE molecules can self-assemble to minimize the exposure of their central groups to water, as in other bolaform amphiphiles.³³ Herein, on the basis of the obviously increased water solubility of STE–RES (Figure 1), it is proposed that hydrophobic RES is encapsulated in the self-assembled STE micelles in water to avoid aqueous environments. Moreover, the formed nanoparticles evidenced by DLS and AFM analyses (data not shown) were also believed to be nanomicelles. To further explore if the micelle formation of STE plays a key role in the solubilization of RES, the CMC of STE in water was determined by the pyrene fluorescent method. The fluorescent spectrum of pyrene is sensitive to its microenvironmental polarity. Upon micellization, pyrene molecules preferably locate inside or close to the hydrophobic core of micelles, and consequently the intensity ratio I_{373}/I_{385} is changed.^{26,27} The results are shown in Figure S2 in the Supporting Information. The CMC value of STE was determined from the threshold concentration, where the pyrene I_{373}/I_{385} begins to change markedly.^{26,27} Therefore, the CMC of STE was determined as 4.94 mg/mL (Supporting Information, Figure S2). Compared with other surfactants and synthetic amphiphilic polymer micelles, STE has a relatively high CMC, which should be attributed to its big portion of hydrophilic sugar units attached to steviol structure.

As expected above, the initial improvement of RES solubility in water solution appeared at above the CMC of STE, as evidenced by RES solubility data (Figure 1). With the above results taken into consideration, it could be speculated that the solubilization of RES in STE solutions should be mainly attributed to the formation of self-assembled STE micelles in water. STE micelles can encapsulate RES by the formation of a water-soluble complex derived from the interaction between hydrophobic cores of STE micelles and the hydrophobic group of RES, resulting in the solubilization of RES in water (Figure 1). A similar finding was described by Zhang et al.,³⁴ who reported that hydrophobic curcumin was solubilized in rubusoside, another kind of steviol glycoside, by the formation of a curcumin–rubusoside nanoparticle.

Interactions between SPI and STE/STE–RES in Aqueous Solution. In this study, we attempted to investigate the effect of STE/STE–RES on the physical properties and oxidative stability of protein-based emulsions. The interactions between protein and other surface active components of the system are usually believed to influence their interfacial adsorption and the formation of viscoelastic films around oil droplets to stabilize the droplets against flocculation and coalescence. Herein, the interactions between SPI and STE/STE–RES in aqueous phase were thus studied to understand the underlying mechanism of emulsion stability. The fluorescence quenching method was used to study the binding reaction between small molecules and proteins. Fluorescence quenching refers to any process that decreases the fluorescence intensity of a sample. A variety of mechanisms can cause quenching, such as excited state reaction, molecular rearrangement, energy transfer, ground state complex formation, and collision quenching. Figure 2A shows the fluorescence emission spectra of SPI with different concentrations of STE. For STE concentrations below 0.8 mg/mL, no obvious changes in the fluorescence intensity of SPI were observed, suggesting that no interaction between SPI and STE occurred. As the concentration of STE was increased from 2 to 20 mg/mL, the addition of STE gave rise to a progressive quenching of the fluorescence of SPI, suggesting that there was interaction between SPI and STE. To further discern the fluorescence quenching mechanism, the Stern–Volmer eq 1 was used for the fluorescence data analysis. As shown in the inset of Figure 2A, the value of k_q is much lower than the maximal dynamic quenching constant ($2.0 \times 10^{10} \text{ M}^{-1} \text{ s}^{-1}$), indicating that the fluorescence quenching induced by STE is dynamic collision quenching.^{28,35}

Figure 2B shows the steady state fluorescence for quenching of SPI in the presence of STE–RES. SPI exhibited a strong fluorescence emission with a peak at around 335 nm. With the increment of STE–RES, a gradual attenuation of the fluorescence intensity of SPI along with a red shift of the maximum emission from 335.2 to 376.6 nm was observed, suggesting that there was strong interaction between SPI and STE–RES complex. Data fitted from Stern–Volmer plots is given in the inset of Figure 2B. It can be seen that the value of k_q is much higher than the maximal dynamic quenching constant ($2.0 \times 10^{10} \text{ M}^{-1} \text{ s}^{-1}$), signifying that the probable quenching mechanism for SPI fluorescence by STE–RES is a static type.^{26,33} These results indicated that STE–RES may bind with aromatic amino acid residues of SPI, forming a SPI–STE–RES ternary complex. This is in agreement with previous studies,^{36,37} which have reported that RES interacts with protein to form a RES–protein complex.

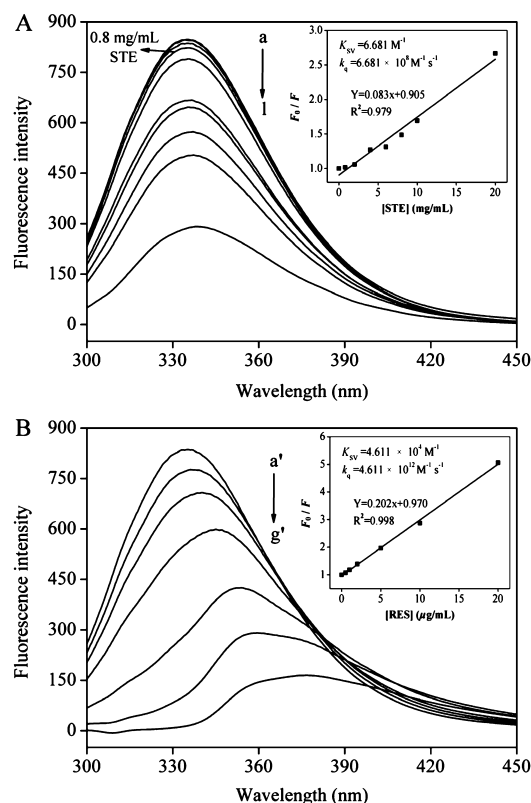


Figure 2. Fluorescence emission spectra of SPI with various amounts of STE (A) and STE–RES (B) in 10 mM phosphate buffer at pH 7.0: (a, a') 0.5 mg/mL SPI alone; (b–l) 0.5 mg/mL SPI with 0.05, 0.1, 0.2, 0.4, 0.8, 2, 4, 6, 8, 10, and 20 mg/mL STE, respectively; (b'–g') 0.5 mg/mL SPI with 0.5, 1, 2, 5, 10, and 20 $\mu\text{g/mL}$ STE–RES, respectively. (Insets) Stern–Volmer plots describing fluorescence quenching of SPI in the presence of STE (A) and STE–RES (B).

Physical Characterization of Emulsions. Particle Size Distribution and Physical Stability. The particle size distributions and changes in the mean droplet diameter (d_{43}) for emulsions stabilized by SPI and STE–RES were used to assess emulsifying ability and physical stability, as shown in Figure 3. The fresh emulsion stabilized by SPI only (control) exhibited a large particle size with d_{43} at $1.28 \mu\text{m}$. Compared to the control, the emulsions in the presence of STE were fine, with a narrow and uniform size distribution (Figure 3A). With increasing STE concentration from 0.4 to 0.8%, a gradual reduction in the d_{43} was observed, suggesting the improvement of emulsifying ability. Moreover, there were no significant differences ($p > 0.05$) in the particle size distributions or d_{43} of emulsions with the addition of RES (between 0.8% STE and 0.8% STE + 0.005–0.02% RES) (Figure 3A). These results indicated that the initial particle properties of SPI-based emulsions were mainly improved due to the presence of STE. The existence of RES in the STE–RES complex could not influence the adsorption of STE at the oil–water interface. These results are in accordance with CLSM observations (Figure 3A, inset).

To evaluate the physical stability of emulsions stabilized by SPI and STE/STE–RES, the changes in the d_{43} of emulsions were followed during storage (Figure 3B). As shown in Figure 3B, a marked increase in d_{43} was observed for the control emulsion with increasing storage time, reaching values of $5.98 \mu\text{m}$ at day 21. Compared to the control, the physical stability of

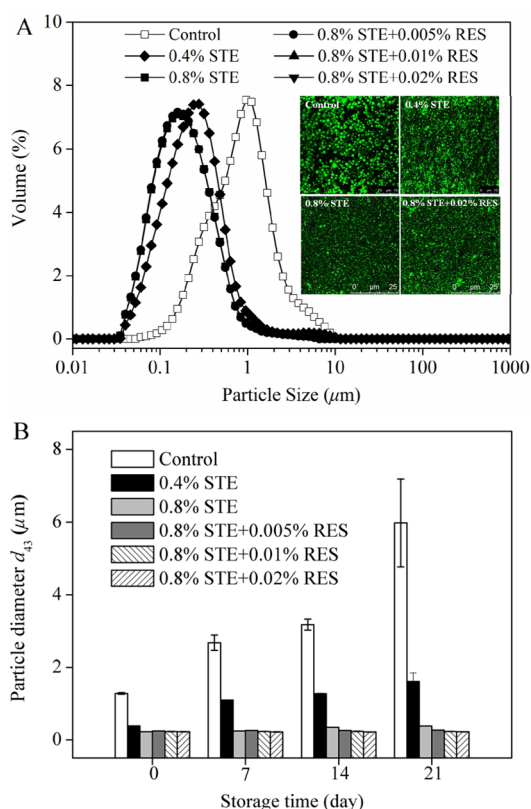


Figure 3. (A) Particle size distributions of fresh emulsions stabilized by SPI and STE/STE–RES complex. (B) Changes in mean particle diameter d_{43} of emulsions during storage for 21 days. Control: SPI-based emulsion. 0.4% STE and 0.8% STE designate SPI-based emulsions with 0.4 and 0.8% STE (w/v), respectively. 0.8% STE + 0.005% RES, 0.8% STE + 0.01% RES, and 0.8% STE + 0.02% RES designate emulsions with 0.8% STE and 0, 0.005, 0.01, and 0.02% (w/v) of RES, respectively.

emulsions in the presence of STE were obviously improved (Figure 3B). With increasing STE concentration to 0.8% (w/v), the d_{43} showed a slight increase to 0.384 μm after 21 days. In addition, no obvious differences were found in the d_{43} of emulsions with the addition of RES (between 0.8% STE and 0.8% STE + 0.005–0.02% RES) during storage (Figure 3B). These results are in good agreement with particle size distributions analysis, indicating that the improvement of physical stability of emulsions should be mainly due to the presence of STE.

Interfacial Protein Adsorption Fraction (F_{ads}) and RES Concentration. Effects of STE and STE–RES on interfacial protein adsorption fraction (F_{ads}) and RES concentration of emulsions are shown in Figure 4. The amphiphilic structure of STE molecules endowed STE with potential capability as natural small surface-active substances, which can rapidly adsorb at the oil–water interface.³⁸ As shown in Figure 4, the control emulsion had a maximum F_{ads} of 39.3%. With increasing STE concentration, the F_{ads} was obviously decreased. Compared to the control (39.3%), the F_{ads} of emulsion stabilized by SPI and STE was 12.2% when STE concentration was increased to 0.8%, representing that more than about 70% of the initial interfacial protein was displaced. These results suggested that the decrease in the amount of SPI adsorbed at the oil–water interface was attributed to the competition for surface space of oil droplets with the more surface-active STE.

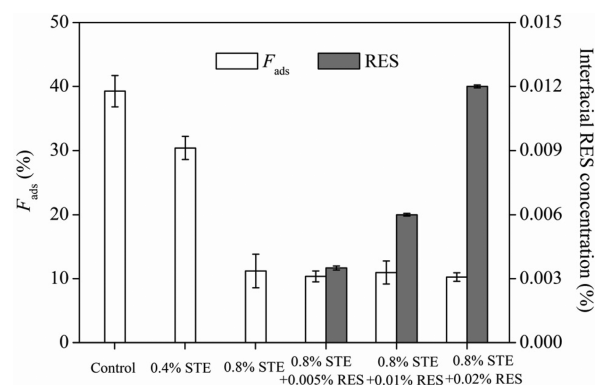


Figure 4. Interfacial protein adsorption fraction (F_{ads}) and RES concentration in aqueous phase of emulsions stabilized by SPI and STE–RES complex. Control, SPI-based emulsion. 0.4% STE and 0.8% STE designate SPI-based emulsions with 0.4 and 0.8% STE (w/v), respectively. 0.8% STE + 0.005% RES, 0.8% STE + 0.01% RES, and 0.8% STE + 0.02% RES designate emulsions with 0.8% STE and 0, 0.005, 0.01, and 0.02% (w/v) of RES, respectively.

Moreover, there were no significant differences ($p > 0.05$) in the F_{ads} of emulsions in the presence of RES (between 0.8% STE and 0.8% STE + 0.005–0.02% RES) (Figure 4), suggesting that the addition of RES had no effect on the F_{ads} . These results further indicated that the interfacial protein displacement was attributed to the addition of STE, consistent with the analysis of particle size distribution and physical stability (Figure 3).

In addition, an increase in concentration of STE–RES resulted in an increase in interfacial RES concentration (Figure 4). All of emulsions containing STE–RES exhibited a high accumulation of RES (around 60% of added RES) at the oil–water interface, which is thought to contribute to improve the antioxidant efficiency of RES in O/W emulsions.^{1,4} As mentioned above, STE can adsorb competitively with SPI into the oil–water interface. Therefore, it is speculated that STE–RES may migrate to the interface, a process that is simultaneously accompanied by the adsorption of STE micelles at the oil–water interface, thus increasing the concentration of RES at the interface. In addition, the ability of STE–RES to bind to interfacial SPI may also have resulted in increased accumulation of RES at the oil droplet surface (Figure 2B).

Enhanced Oxidative Stability of Emulsions. With the fact of increasing RES adsorption at the oil–water interface taken into consideration, the oxidative stability of emulsions stabilized by SPI and STE/STE–RES was further studied, as shown in Figure 5. Lipid hydroperoxides, generally accepted as the first oxidation products, were measured to observe the initial oxidation rate of emulsions. Compared to hydroperoxides of SPI emulsion (control), it is interesting to note that the 0.8% STE emulsion showed a lower level of hydroperoxides during storage (Figure 5A). For emulsions containing STE–RES, lipid hydroperoxides were markedly lower compared to the control and 0.8% STE emulsion. Furthermore, higher STE–RES concentrations led to lower hydroperoxides, indicating higher oxidative stability of emulsions. Compared with the control (109.9 mmol/kg oil) and 0.8% STE emulsion (75.9 mmol/kg oil), the highest concentration of STE–RES (0.02%) led to the lowest level of hydroperoxides (40.9 mmol/kg oil). These results indicated that STE–RES displayed an effective inhibition in the formation of lipid hydroperoxides.

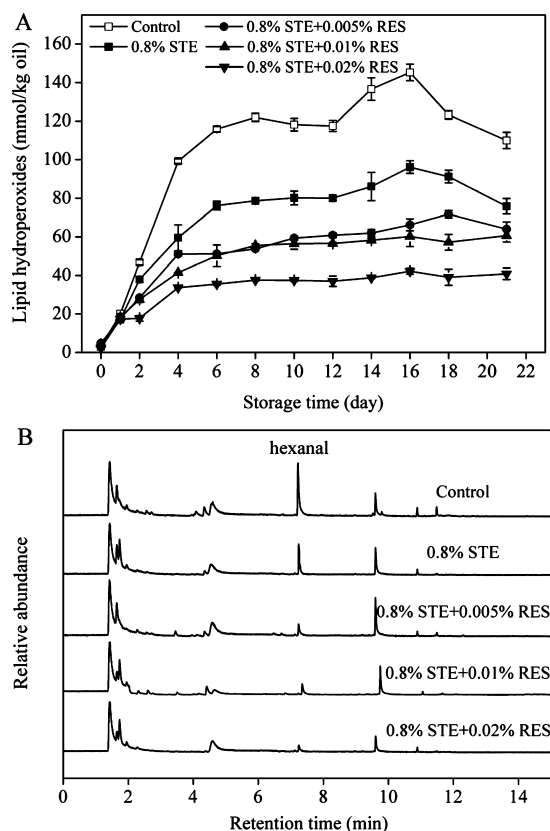


Figure 5. Changes in lipid hydroperoxides (A) and headspace hexanal (B) of emulsions stabilized by SPI and STE-RES complex during storage at 37 °C for 21 days. Control, SPI-based emulsion. 0.8% STE designates SPI-based emulsion with 0.8% STE (w/v). 0.8% STE + 0.005% RES, 0.8% STE + 0.01% RES, and 0.8% STE + 0.02% RES designate emulsions with 0.8% STE and 0, 0.005, 0.01, and 0.02% (w/v) of RES, respectively.

Furthermore, the volatile compounds produced after 21 days were analyzed by headspace analysis (Figure 5B). There was a complex mixture of secondary oxidation products formed during lipid oxidation, and hexanal is a major secondary oxidation product of corn oil. The whole chromatograms are shown with one identified peak for hexanal and other peaks corresponding to the unidentified oxidation products. After 21 days of storage, SPI emulsion (control) exhibited a large peak area of hexanal (1.3×10^9). The presence of 0.8% STE reduced the hexanal peak area of emulsion to 5.3×10^8 when compared with the control (Figure 5B). For emulsions containing STE-RES, with increasing STE-RES concentrations, a gradual decrease was found for the peak area of hexanal in emulsions. The peak area of hexanal for 0.8% STE + 0.02% RES emulsion was 1.48×10^8 , which was markedly lower than that of the control (1.3×10^9) and 0.8% STE emulsion (5.3×10^8). These results were in good agreement with those obtained from lipid hydroperoxides results (Figure 5A) and provided further evidence that STE-RES effectively improved the oxidative stability of emulsions. A similar finding was obtained by Medina et al.,¹² who found that around 0.005–0.01% RES had a significant effect of improving oxidative stability in fish oil-based emulsion prepared with lecithin as an emulsifier.

General Discussion. In this work, compared to control emulsion, the addition of STE distinctly improved the stability of SPI-based emulsion, especially the physical stability (Figure 3). Moreover, the incorporation of STE-RES in protein

emulsion could also lead to further obvious enhancement of emulsion oxidative stability (Figures 3 and 5). To clarify a reasonable understanding of enhanced physical and oxidative stabilities, a schematic illustration of the formation of SPI-based emulsion with STE-RES is proposed and shown in Figure 6.

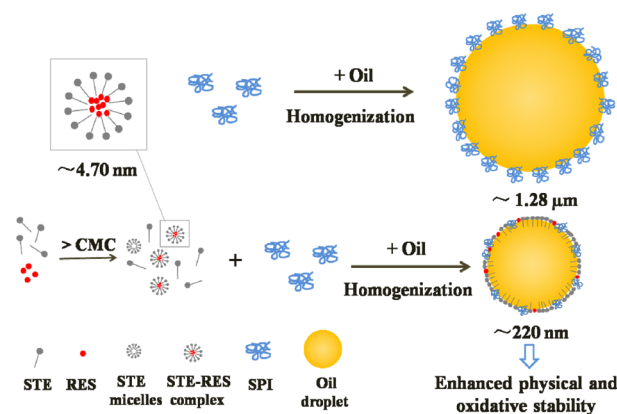


Figure 6. Schematic illustration of the formation of O/W emulsion stabilized by SPI and STE-RES.

RES, the stilbenoid that shows a resonance structure, has poor solubility in aqueous and lipid phases (Figure S1 in the Supporting Information). STE is an amphiphilic compound possessing both a hydrophobic steviol backbone and hydrophilic glucosyl and sophorosyl residues (Figure S1 in the Supporting Information). The STE molecule has the shape of bolaamphiphiles that have hydrophobic rings in the center with hydrophilic hydroxyl groups on each end (Figure S1 in the Supporting Information). The shape of the STE molecule can drive it to self-assemble, minimizing the exposure of its central groups to water. Thus, hydrophobic RES might be encapsulated in the self-assembled STE micelles (~4.70 nm) to avoid aqueous environments when the STE concentration is above its CMC (Figures 1 and 6). During the homogenizing process, SPI and STE/STE-RES in the aqueous phase would competitively adsorb into the oil–water interface of emulsions. This behavior was supported by the determination of a protein adsorption fraction (F_{ads}), where about 70% of the initial interfacial SPI was displaced by the addition of 0.8% STE (Figures 4 and 6). The existence of RES did not influence the adsorption amount of SPI and STE (Figure 4). These results indicated that STE probably played a predominant role in the improvement of emulsion physical stability. The fast adsorption of STE at the oil–water interface endowed the emulsion with a smaller oil droplet size (~220 nm) and a higher physical stability (Figures 3 and 6). These phenomena may be attributed to the formation of a compact mixed SPI-STE interface membrane around the oil droplets.

It is generally considered that lipid oxidation in O/W emulsion systems is thought to occur at the oil–water interface because the oxidation substrate, lipid hydroperoxides, are surface active and therefore accumulate at the oil–water interface.^{1,3} Lipid hydroperoxides can be decomposed into free radicals by pro-oxidants such as transition metals.^{1,3} On the basis of these understandings, how to inhibit interfacial oxidation may mainly determine the oxidative stability of emulsions. Generally, the phenolic antioxidants could capture free radicals by donation of phenolic hydrogen atoms to block the lipid radical reactions. This may be one of the dominant

antioxidation mechanisms of RES in emulsion systems. In the case of mixed emulsion systems, STE-RES may migrate to the interface during the adsorption of STE micelles at the oil-water interface, thus resulting in a high interfacial RES concentration (Figures 4 and 6). In addition, the binding of STE-RES with interfacial SPI may also contribute to the increase in interfacial RES concentration (Figure 2). The high accumulation of RES at the interface would increase the ability of RES to scavenge free radicals produced from the decomposition of interfacial lipid hydroperoxides.^{1,3}

It is notable that STE could improve the oxidation stability of protein emulsions to some extent (Figure 5). However, this information appears to be contradictory to the fact that STE has a limited antioxidant capacity according to the ORAC assay (data not shown). Because the 0.8% STE in emulsions was above its CMC, it is possible that the presence of STE micelles in emulsions could contribute to the inhibition of lipid oxidation. Cho et al.³⁹ found that the presence of surfactant micelles could solubilize iron and remove it from emulsion droplets, thus inhibiting the lipid oxidation. Moreover, surfactant micelles can also solubilize lipid hydroperoxides out of emulsions droplets, which can decrease free radicals in the oil droplets due to hydroperoxide decomposition.⁴⁰ In addition, a mixed SPI-STE interface membrane around the oil droplets, as speculated in the improvement of physical stability (Figures 3 and 4), may be another possible reason for enhanced oxidation stability of SPI-based emulsions in the presence of STE. It is speculated that such a compact interfacial membrane may act as an effective barrier to the diffusion of lipid oxidation initiators into the oil droplets and then inhibit the formation of lipid radicals by limiting the interaction between transition metals in the aqueous phase and the oil phase.^{1,3}

In conclusion, a water-soluble RES was fabricated by the encapsulation of RES in STE self-assembled micelles. The physical properties and oxidative stability of SPI-based O/W emulsion systems were enhanced by the incorporation of STE-RES. The enhanced physical properties of emulsions were mainly related to the formation of mixed interfacial layers caused by competitive interfacial adsorption between SPI and STE. Meanwhile, higher interfacial accumulation of RES was mainly responsible for enhanced antioxidant efficiency of RES in emulsions. These findings revealed that hydrophobic polyphenols, such as RES, could be used as efficient antioxidants in O/W emulsions by the utilization of solubilizing properties and notable surface activity of STE. This would provide a good model for designing stable emulsified food systems with enhanced physical and oxidative stabilities.

■ ASSOCIATED CONTENT

Supporting Information

Structures of RES and STE (Figure S1) and critical micelle concentration measurement of STE (Figure S2). This material is available free of charge via the Internet at <http://pubs.acs.org>.

■ AUTHOR INFORMATION

Corresponding Author

*E-mail: fexqyang@scut.edu.cn. Phone: (086) 20-87114262. Fax: (086) 20-87114263.

Funding

This research was supported by grants from the Chinese National Natural Science Foundation (serial no. 31130124) and the Project of National Key Technology Research and

Development Program for the 12th Five-year Plan (2012BAD33B10, 2012BAD34B04-2).

Notes

The authors declare no competing financial interest.

■ REFERENCES

- (1) McClements, D. J.; Decker, E. A. Lipid oxidation in oil-in-water emulsions: impact of molecular environment on chemical reactions in heterogeneous food systems. *J. Food Sci.* **2000**, *65*, 1270–1282.
- (2) Shahidi, F.; Zhong, Y. Lipid oxidation and improving the oxidative stability. *Chem. Soc. Rev.* **2010**, *39*, 4067–4079.
- (3) Waraho, T.; McClements, D. J.; Decker, E. A. Mechanisms of lipid oxidation in food dispersions. *Trends Food Sci. Technol.* **2011**, *22*, 3–13.
- (4) Frankel, E. N.; Huang, S. W.; Kanner, J.; German, J. B. Interfacial phenomena in the evaluation of antioxidants: bulk oils vs. emulsions. *J. Agric. Food Chem.* **1994**, *42*, 1054–1059.
- (5) Brewer, M. S. Natural antioxidants: sources, compounds, mechanisms of action, and potential applications. *Compr. Rev. Food Sci. Food Saf.* **2011**, *10*, 221–247.
- (6) Vang, O.; Ahmad, N.; Baile, C. A.; Baur, J. A.; Brown, K.; Csiszar, A.; Das, D. K.; Delmas, D.; Gottfried, C.; Lin, H. Y.; Ma, Q. Y.; Mukhopadhyay, P.; Nalini, N.; Pezzuto, J. M.; Richard, T.; Shukla, Y.; Surh, Y. J.; Szekeres, T.; Szekudelski, T.; Walle, T.; Wu, J. M. What is new for an old molecule? Systematic review and recommendations on the use of resveratrol. *PLoS One* **2011**, *6*, e19881.
- (7) Kimura, Y.; Ohminami, H.; Okuda, H.; Baba, K.; Kozawa, M.; Arichi, S. Effects of stilbene components of roots of *Polygonum* ssp. on liver injury in peroxidized oil-fed rats. *Planta Med.* **1983**, *49*, 51–54.
- (8) Sánchez-Moreno, C.; Larrauri, J. A.; Saura-Calixto, F. Free radical scavenging capacity and inhibition of lipid oxidation of wines, grape juices and related polyphenolic constituents. *Food Res. Int.* **1999**, *32*, 407–412.
- (9) Wang, M.; Jin, Y.; Ho, C.-T. Evaluation of resveratrol derivatives as potential antioxidants and identification of a reaction product of resveratrol and 2,2-diphenyl-1-picrylhydrazyl radical. *J. Agric. Food Chem.* **1999**, *47*, 3974–3977.
- (10) Gülçin, I. Antioxidant properties of resveratrol: a structure-activity insight. *Innovative Food Sci. Emerging Technol.* **2010**, *11*, 210–218.
- (11) Soares, D. G.; Andreazza, A. C.; Salvador, M. Sequestering ability of butylated hydroxytoluene, propyl gallate, resveratrol, and vitamins C and E against ABTS, DPPH, and hydroxyl free radicals in chemical and biological systems. *J. Agric. Food Chem.* **2003**, *51*, 1077–1080.
- (12) Medina, I.; Alcántara, D.; González, M. J.; Torres, P.; Lucas, R.; Roque, J.; Plou, J. F.; Morales, J. C. Antioxidant activity of resveratrol in several fish lipid matrices: effect of acylation and glucosylation. *J. Agric. Food Chem.* **2010**, *58*, 9778–9786.
- (13) Filip, V.; Plocková, M.; Šmidrkal, J.; Špičková, Z.; Melzoch, K.; Schmidt, S. Resveratrol and its antioxidant and antimicrobial effectiveness. *Food Chem.* **2003**, *83*, 585–593.
- (14) Lee, M. H.; Kao, L.; Lin, C. C. Comparison of the antioxidant and transmembrane permeative activities of the different *Polygonum cuspidatum* extracts in phospholipid-based microemulsions. *J. Agric. Food Chem.* **2011**, *59*, 9135–9141.
- (15) Laguerre, M.; López-Girald, L. J.; Lecom, J.; Figueroa-Espinoza, M. J.; Baréa, B.; Weiss, J.; Decker, E. A.; Villeneuve, P. Chain length affects antioxidant properties of chlorogenate esters in emulsion: the cut-off theory behind the polar paradox. *J. Agric. Food Chem.* **2009**, *57*, 11335–11342.
- (16) Lucas-Abellan, C.; Fortea, M. I.; Gabaldon, J. A.; Nunez-Alecio, E. Complexation of resveratrol by native and modified cyclodextrins: determination of complexation constant by enzymatic, solubility and fluorimetric assays. *Food Chem.* **2008**, *111*, 262–267.
- (17) Sessa, M.; Tsao, R.; Liu, R. H.; Ferrari, G.; Donsì, F. Evaluation of the stability and antioxidant activity of nanoencapsulated resveratrol during in vitro digestion. *J. Agric. Food Chem.* **2011**, *59*, 12352–12360.

- (18) Atanackovic, M.; Posa, M.; Heinle, H.; Gojkovic-Bukarica, L.; Cvejić, J. Solubilization of resveratrol in micellar solutions of different bile acids. *Colloids Surf. B: Biointerfaces* **2009**, *72*, 148–154.
- (19) Zhijun, L. Diterpene glycosides as natural solubilizers. PCT/US2009/040324, 2010; pp 10–15.
- (20) Geuns, J. M. C. Stevioside. *Phytochemistry* **2003**, *64*, 913–921.
- (21) Hsieh, M. H.; Chan, P.; Sue, Y. M.; Liu, J. C.; Liang, T. H.; Huang, T. Y.; Tomlinson, B.; Chow, M. S. S.; Kao, P. F.; Chen, Y. J. Efficacy and tolerability of oral stevioside in patients with mild essential hypertension: a two-year, randomized, placebo-controlled study. *Clin. Ther.* **2003**, *25*, 2797–2808.
- (22) Chan, P.; Tomlinson, B.; Chen, Y. J.; Liu, J. C.; Hsieh, M. H.; Cheng, J. T. A double-blind placebo-controlled study of the effectiveness and tolerability of oral stevioside in human hypertension. *Br. J. Clin. Pharmacol.* **2000**, *50*, 215–220.
- (23) Yasukawa, K.; Kitanaka, S.; Seo, S. Inhibitory effect of stevioside on tumor promotion by 12-*O*-tetradecanoylphorbol-13-acetate in two-stage carcinogenesis in mouse skin. *Biol. Pharm. Bull.* **2002**, *25*, 1488–1490.
- (24) Boonkaewwan, C.; Toskulkao, C.; Vongsakul, M. Anti-inflammatory and immunomodulatory activities of stevioside and its metabolite steviol on THP-1 cells. *J. Agric. Food Chem.* **2006**, *54*, 785–789.
- (25) Wang, J.-M.; Xia, N.; Yang, X.-Q.; Yin, S.-W.; Qi, J.-R.; He, X.-T.; Yuan, D.-B.; Wang, L.-J. Adsorption and dilatational rheology of heat-treated soy protein at the oil-water interface: relationship to structural properties. *J. Agric. Food Chem.* **2012**, *60*, 3302–3310.
- (26) Aguiar, J.; Carpena, P.; Molina-Bolívar, J. A.; Ruiz, C. C. On the determination of the critical micelle concentration by the pyrene 1:3 ratio method. *J. Colloid Interface Sci.* **2003**, *258*, 116–122.
- (27) Mravec, F.; Pekař, M.; Velebný, V. Aggregation behavior of novel hyaluronan derivatives – a fluorescence probe study. *Colloid Polym. Sci.* **2008**, *286*, 1681–1685.
- (28) Lakowicz, J. R. *Principles of Fluorescence Spectroscopy*, 3rd ed.; Springer Science + Business Media: New York, 2006.
- (29) Akhtar, M.; Dickinson, E.; Mazoyer, J.; Langendorff, V. Emulsion stabilizing properties of depolymerised pectin. *Food Hydrocolloids* **2002**, *16*, 249–256.
- (30) Panya, A.; Laguerre, M.; Lecomte, J.; Villeneuve, P.; Weiss, J.; McClements, D. J.; Decker, E. A. Effects of chitosan and rosmarinic esters on the physical and oxidative stability of liposomes. *J. Agric. Food Chem.* **2010**, *58*, 5679–5684.
- (31) Tong, L. M.; Sasaki, S.; McClements, D. J.; Decker, E. A. Antioxidant activity of whey in a salmon oil emulsion. *J. Food Sci.* **2000**, *65*, 1325–1329.
- (32) Sabadini, E.; Cosgrove, T.; Egidio, F. d. C. Solubility of cyclomaltooligosaccharides (cyclodextrins) in H₂O and D₂O: a comparative study. *Carbohydr. Res.* **2006**, *341*, 270–274.
- (33) Claussen, R. C.; Rabatic, B. M.; Stupp, S. I. Aqueous self-assembly of unsymmetric peptide bolaamphiphiles into nanofibers with hydrophilic cores and surfaces. *J. Am. Chem. Soc.* **2003**, *125*, 12680–12681.
- (34) Zhang, F.; Gar, Y. K.; Duane, P. J.; Javoris, H.; Pauls, R.; Graca, V.; Rhett, W. S.; Liu, Z. J. A novel solubility-enhanced curcumin formulation showing stability and maintenance of anticancer activity. *J. Pharm. Sci.* **2011**, *100*, 2778–2789.
- (35) Bi, S. Y.; Ding, L.; Tian, Y.; Song, D. Q.; Zhou, X.; Liu, X.; Zhang, H. Q. Investigation of the interaction between flavonoids and human serum albumin. *J. Mol. Struct.* **2004**, *703*, 37–45.
- (36) Liang, L.; Tajmir-Riahi, H. A.; Muriel, S. Interaction of β -lactoglobulin with resveratrol and its biological implications. *Biomacromolecules* **2008**, *9*, 50–56.
- (37) Bourassa, P.; Kanakis, C. D.; Tarantilis, P.; Pollissiou, M. G.; Tajmir-Riahi, H. A. Resveratrol, genistein, and curcumin bind bovine serum albumin. *J. Phys. Chem. B* **2010**, *114*, 3348–3354.
- (38) Demetriades, K.; McClements, D. J. Influence of pH and heating on physicochemical properties of whey protein-stabilized emulsions containing a nonionic surfactant. *J. Agric. Food Chem.* **1998**, *46*, 3936–3942.
- (39) Cho, Y.-J.; McClements, D. J.; Decker, E. A. Ability of surfactant micelles to alter the physical location and reactivity of iron in oil-in-water emulsions. *J. Agric. Food Chem.* **2002**, *50*, 5704–5710.
- (40) Nuchi, C. D.; Hernandez, P.; McClements, D. J.; Decker, E. A. Ability of lipid hydroperoxides to partition into surfactant micelles and alter lipid oxidation rates in emulsions. *J. Agric. Food Chem.* **2002**, *51*, 5522–5527.